PROPERTIES OF A DOUBLE MAGNETIC SUSPENSION

B.E. BERNARD, W.S. CHEUNG, AND R.C. RITTER

DEPARTMENT OF PHYSICS, UNIVERSITY OF VIRGINIA

CHARLOTTESVILLE, VIRGINIA 22901 U.S.A.

in

Proceedings of the 1983 International School and Symposium on Precision Measurement and Gravity Experiment, Taipei, Republic of China, January 24 - February 2, 1983, ed. by W.-T. Ni (Published by National Tsing Hua University, Hsinchu, Taiwan, Republic of China, June, 1983)

OUTLINE

I. Introduction 105

II. Shroud Rotor Suspension 106

III. Proof Rotor Suspension 107

IV. Double Magnetic Suspension 110

V. Conclusion 116

References 117

PROPERTIES OF A DOUBLE MAGNETIC SUSPENSION*

B. E. Bernard, W. S. Cheung,** and R. C. Ritter

Department of Physics, University of Virginia
Charlottesville, VA 22901 USA

I. Introduction

The final usefulness of precision rotors as special tools for experimental gravitation will depend on their ultimate stability. The more common means of protection against magnetic, electrical, vibrational, acoustic, etc. interference as used for many kinds of precision measurement are needed here. But in addition, two particular rotation problems must be solved: the finite drag rotors experience as a result of bearing friction and because of gas drag. This paper discusses the particular magnetic bearing which applies to solutions of both these sources of friction. This "double magnetic suspension" is being developed in connection with an inertial clock which uses an ultra-free rotor as its basic oscillator.

In assessing the need for special friction-reducing techniques we can look at some classical cases. The earth, because of tidal and other possible couplings.[1,2], and because of its unsolid composition, is not as free as laboratory rotors potentially are. Its decay time (to 1/e of a given initial angular velocity) is estimated at 3 to 4 billion years from geological data[3] and may be varying with time. There is even the hint that motion of our solar system across the galaxy arms may influence this rotation.[4]

Laboratory rotors, though stiffer and potentially more uniform, have the gas and bearing drag mentioned already. For rotors of a few cm diameter the gas-limited decay time τ^* is roughly[5] 100/P, where P is the pressure in Torr. Thus for $\tau^* \geq 10^{18}$s, P must be $\leq 10^{-16}$ Torr, an unachievably low value in the laboratory. In the mm-sized rotors of Beams[5,6] and Fremery[7] gas drag was nearly always the limiting factor, although Fremery probably also observed the tiny unavoidable eddy current drag associated with ferromagnetic suspensions.

Beams[8] (or perhaps Alvarez) first suggested the reduction of gas drag by moving the gas around with the rotor and he developed the first double magnetic suspension for this purpose. This, however, was done several decades ago, when stable instrumentation was not available to him, and the properties of the double suspension were never studied beyond the functioning of the method.

The present experiment corotates the gas (at low pressures well into the free-molecule regime) by corotating an outer, shroud, rotor. Sensors detect the angular position of both the shroud and inner, proof rotor. A computer-controlled servomechanism keeps the shroud rotor synchronous with the proof rotor. Details of this operation are given in another paper at this symposium.[9]

A further aspect guiding our design is the need for larger, slower rotors than those of Beams and Fremery. Such rotors are much less subject to drift from centrifugal stress than the earlier small ones. Concomittant with this is the use of period, rather than frequency measurement of the speed, and related averaging strategies to minimize instrumental error as well as measurement and control error due to rotor random walk[10].

Another corotation scheme, without feedback, has been developed in our laboratory[1,11]. It differs also in scale, in rotor shape, in many design details and features. But it differs particularly in using a hybrid double suspension--gas bearing for the outer rotor with a magnetic suspension for the inner. While for that corotation scheme the gas bearing is adequate, it has been measured to be many orders of magnitude rougher than the magnetic suspension. As such it would create considerably more severe problems for our servoed corotation scheme.

In the following we describe the strategy, design and properties of the individual two magnetic suspensions, outer and inner, and their functioning together as a double suspension.

II. Shroud Rotor Suspension

The primary property needed of the upper suspension is that it be strong and stable. Our most highly developed split-diode optically-sensed system was used for this. It has been described in detail[12,13]. A particularly useful feature is the one of synchronously detected ac light as a stabilizing feature as well as for protection against varying ambient light.

In this scheme a light-emitting diode is driven with 10 kHz pulses. The pulsed light is focussed to an annulus around the spherical suspension slug (12.7 mm dia. steel ball). The transmitted light passes through a converging lens to the surface of a horizontally split photodiode. The difference signal is amplified and fed to a phase-lock amplifier, referenced to the 10 kHz pulses driving the led, and acting as a synchronous detector. The dc output of this detector feeds the remaining amplifying chain of a conventional type for magnetic suspension[13]. A 40 ms derivative time constant is used.

It is worth mentioning that the power amplifier driving the suspension coil is used in the voltage drive mode. In this and other experiments we have also used the current drive mode, which improves the servo performance of the suspension by essentially eliminating a pole due to the suspension coil inductance. The location of this pole is a common problem and it reduces the loop phase stability margin. Nevertheless, even though the suspension becomes easier to use with current drive, this is often at the expense of increased reaction to ambient vibration. We are still studying this question.

The purpose of using a split photodiode is to have the sensitive, noise- and drift-prone front end circuitry be differential in character so that some of these faults cancel out.

An amplitude spectrum of the preamplifier signal for the upper suspension under typical operating conditions is shown in Fig. 1. This can be regarded as the transfer function of this suspension since the system is driven essentially by wide-band noise. Its salient feature is the resonant-like peak which is characteristic of all our suspensions, which can be modelled as damped harmonic oscillators. This has a peak frequency of 27 Hz and a width corresponding to $Q = 6.9$. Since the mass of the suspended system is ~ 240 gm the inferred spring constant of the suspension is about $k = 7 \times 10^6$ dyne/cm and the damping coefficient is $b = 5.8 \times 10^3$ dyne-s/cm. By attaching small weights and observing the lowering of the rotor with a telescope, a difficult procedure, the value of the spring constant was statically confirmed to within 50%.

III. Proof Rotor Suspension

To avoid inter-rotor suspension coupling from unavoidably scattered light, a hybrid magnetic suspension is used, in which the lower rotor uses a non-optical position sensor. This sensor is a new scheme, the FM-coil modulated sensor.[14,15] In this the proximity of the lower rotor modulates the inductance of a coil in an oscillator and hence the oscillator frequency. This is much more stable than the Q-coil method of Beams,[16] in which the amplitude is modulated as the Q changes.

In our method the ~ 960 kHz oscillator signal is beat against a stable 1.0 MHz reference and the filtered difference is converted to voltage with a f-v converter. The output of this is the sensor output, fed to conventional amplifying circuitry. The sensitivity is about $\Delta f/\Delta z = 140$ kHz/cm and leads, after conversion, to a transfer function $\Delta V/\Delta z = 10.9$ V/cm.

A ferrite rod, 1.25 cm dia. and 3.8 cm long, with a nylon disc 3.8 cm dia. at its waist forms the proof rotor, which has a mass of 26 gm. The nylon disc serves both to mechanically stabilize rotation and as a catcher to prevent contact against the pole piece during initial magnetic pickup of the rotor.

The "amplitude transfer function" of this suspension is shown in Fig. 2. Since this is necessarily a much weaker suspension than the upper, for reasons given in the next section, it's spectrum is more prone to ambient vibration peaks present on the vibration-isolated table. This is the case, since noise is the driver for this spectrum. In addition, several spurious peaks present are presumed to be from twisting modes about a horizontal axis of the rotor.

The peak frequency is 14 Hz, from which $k = 2 \times 10^5$ dyne/cm. The Q of the lower suspension is measured to be 4.7 from the width of the resonance peak. This gives a vaue of 500 dyne-s/cm for the damping coefficient. The value of the spring constant was confirmed to within 50% using the static load method of measuring the spring constant.

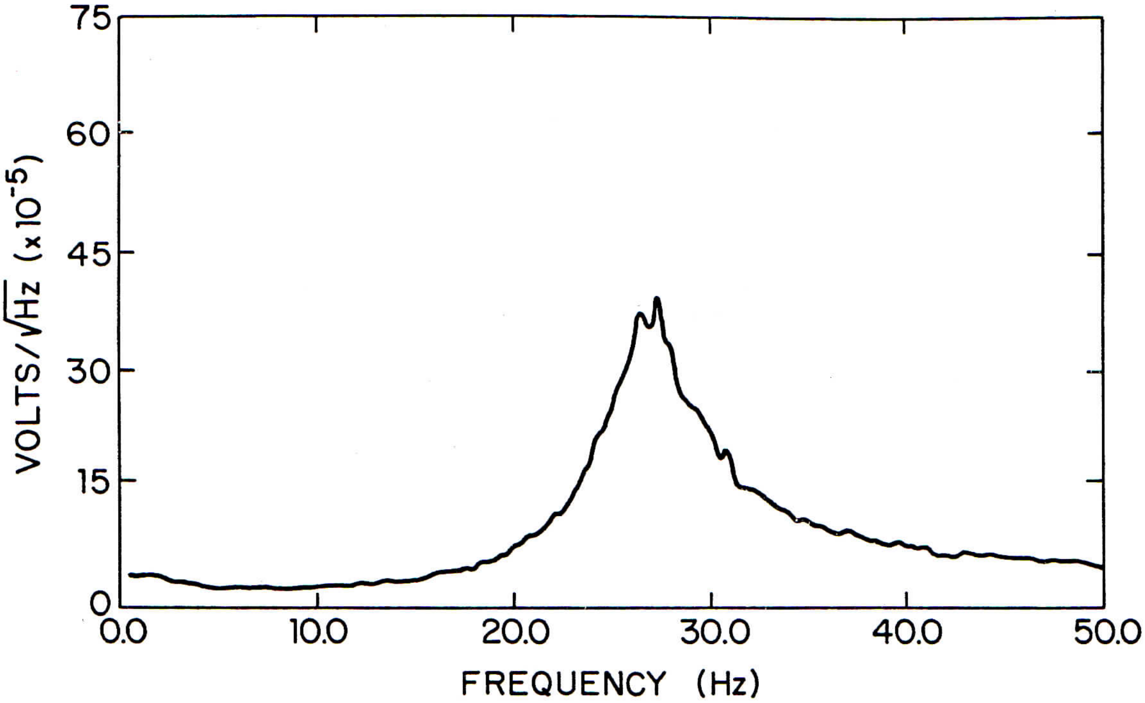

Fig. 1 Measured voltage spectrum of output of the lock-in amplifier which is used as part of the upper suspension position transducer while the suspension is in operation without the lower rotor. From the resonance frequency and width of the resonance peak the spring constant, damping coefficient and Q of the suspension can be calculated. The analyzer bandwidth was 300 mHz.

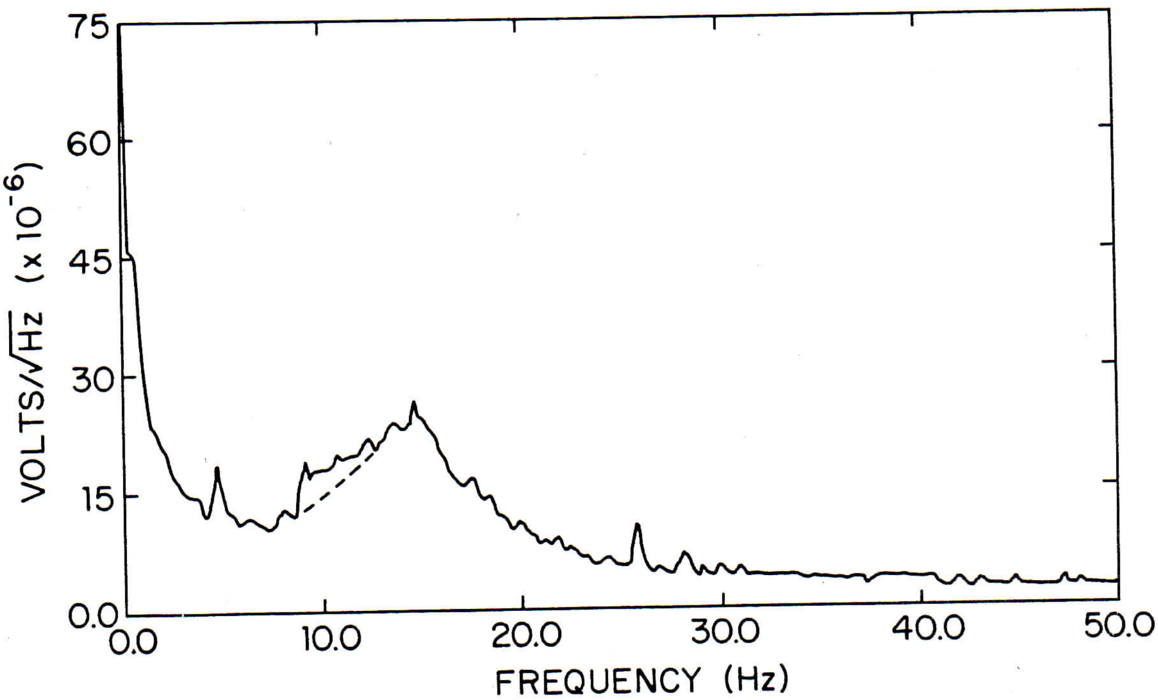

Fig. 2 Measured voltage spectrum of the output of the FM position transducer for the lower suspension while in operation with the upper suspension damped. The peak at ~ 26 Hz is due to vibrations from other equipment in the laboratory. The peaks at 5 Hz and 10 Hz are thought to be due to twisting modes of the suspended object about a horizontal axis. The analyzer bandwidth was 300 mHz.

IV. Double Magnetic Suspension

Just as the individual suspensions can be modelled as damped harmonic oscillators the double suspension can be modelled as two coupled damped harmonic oscillators. Two masses coupled to each other and to the pole pieces by springs and dashpots (representing damping) as shown in Fig. 3 is an appropriate model of the system. The main source of damping comes from the electronic suspension circuitry and can be adjusted so that the motions of the rotors are critically damped. All other sources of damping are negligible. There is no electronic damping between the rotors so b_2 in Fig. 3 is taken to be zero.

The center spring has a negative spring constant (k_2) because of the nature of the magnetic force between the rotors. The spring constants k_1 and k_3 are each due to a combination of negative and positive springs. The negative springs are again due to the nature of the magnetic force between the rotors and their respective pole pieces. The positive springs are a result of the electronic feedback and must be large enough in magnitude so that both k_1 and k_3 are net positive.[17]

Such a system would have many degrees of freedom. It is worth noting that different schemes of double suspension are possible.[8] The particular choice taken here minimizes the inter-rotor coupling.[13]

The rotors are not rigidly fixed in the directions normal to the vertical and the axis of symmetry through each rotor is not confined to the vertical. However, in a well designed system these motions will be exceedingly small. The rotors of course are free to rotate about their vertical axes as required by the nature of the inertial clock. For well designed rotors and position sensing detectors the rotation of the rotors should not couple significantly into the vertical motions. We now consider a system where the rotors are free to move only in the vertical direction.

The response of the masses in Fig. 3 to a driving force applied to the upper mass is now derived. The equations of motion are

$$m_1\ddot{z}_1 + b_1\dot{z}_1 + (k_1 + k_2)z_1 - k_2z_2 = F_o e^{i\omega t} \tag{1}$$

and

$$m_2\ddot{z}_2 + b_3\dot{z}_2 + (k_2+k_3)z_2 - k_2z_1 = 0, \tag{2}$$

where k_2 is a negative number and $F_o e^{i\omega t}$ is a driving force applied to m_1. The solution of Eq. (1) for z_1 with substitution into Eq. (2) assuming $z_2 = A_2e^{i\omega t}$ for the steady-state solution yields,

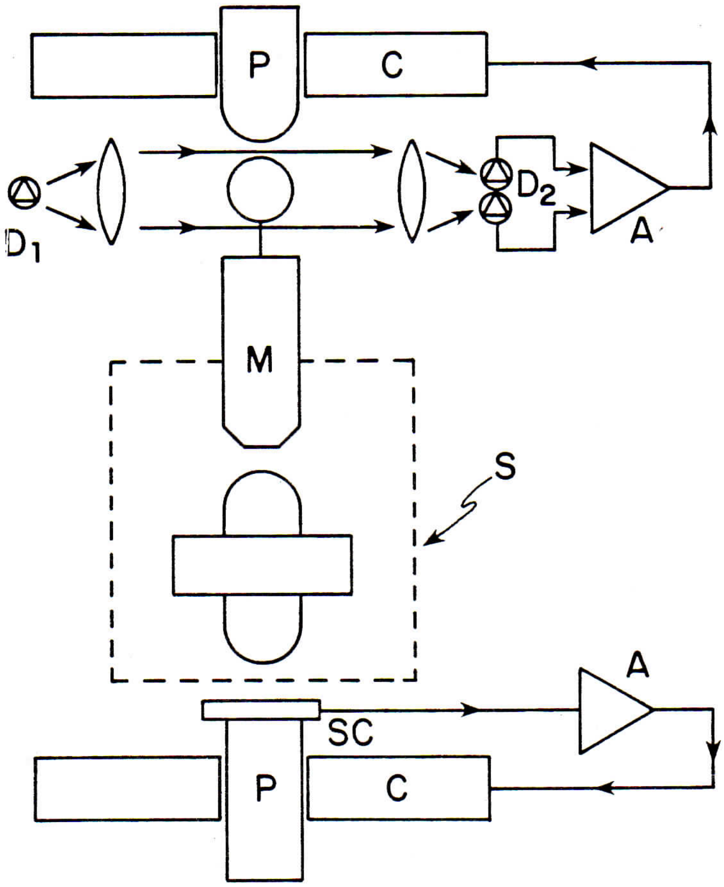

(a)

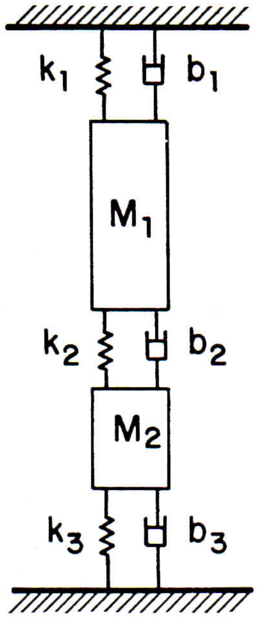

(b)

Fig. 3 (a) Schematic diagram of the double magnetic suspension: coils c, pole-pieces P, LED D_1, split photo-diode D_2, amplifier-derivative A, permanent magnet M, shroud S, sensing coil SC.

(b) Model of the double magnetic suspension as two masses with springs and damping.

$$\{m_1 m_2 \omega^4 - [m_1(k_2+k_3) + m_2(k_1+k_2) + b_1 b_3]\omega^2$$
$$+ (k_1+k_2)(k_2+k_3) - k_2^2 + i[-(m_1 b_3 + m_2 b_1)\omega^3$$
$$+ (b_1(k_2+k_3) + b_3\ (k_1+k_2))\omega]\}\ A_2 = k_2 F_o. \tag{3}$$

The solution of Eq. (3) for $|A_2|$ is an equation relating the amplitude of the steady-state oscillation to the magnitude and frequency of the driving force,

$$|A_2| = F_o \cdot |k_2| \cdot \{[m_1 m_2 \omega^4 - (m_1(k_1+k_2) + m_2(k_2+k_3)+b_1 b_3)\omega^2$$
$$+ (k_1+k_2)(k_2+k_3) - k_2^2]^2 + [-(m_1 b_3 + m_2 b_1)\omega^3$$
$$+ (b_1(k_2+k_3) + b_3(k_1+k_2))\omega]^2\}^{-1/2}. \tag{4}$$

Similarly the amplitude of the upper mass is given by,

$$|A_1| = F_o\{[m_2\omega^2 - (k_2+k_3)]^2 + (b_3\omega)^2\}^{1/2}$$
$$\cdot\{[m_1 m_2 \omega^4 - (m_1(k_1+k_2) + m_2(k_2+k_3) + b_1 b_3)\omega^2$$
$$+ (k_1 + k_2)\ (k_2 + k_3) - k_2^2]^2$$
$$+ [-(m_1 b_3 + m_2 b_1)\omega^3 + (b_1(k_2+k_3) + b_3(k_1 + k_2))\omega]^2\}^{-1/2}. \tag{5}$$

These equations give response curves which are similar to those measured with a spectrum analyzer of the double suspension when appropriate values for the constants (m_1,m_2, k_1, k_3, b_1, b_3) are used. A value for k_2 which yields good results must be assumed since it has not been measured in any other manner.

The measured spectra of the position transducer outputs with the rotors doubly suspended are shown in Fig. 4. The rotors are suspended at the same equilibrium positions as were used for the spectra in Figs. 1 and 2.

The spectrum of the upper suspension is only influenced slightly by the presence of the lower rotor suspended below it. This is to be expected because it is necessary to make the upper suspension much stiffer than the lower suspension in order to realize a stable double suspension. Also, the mass of the lower rotor is only 11% of the mass of the upper rotor.

The resonance peak of the upper suspension shifted slightly upward from 27 Hz to 28 Hz and its amplitude remained essentially unchanged

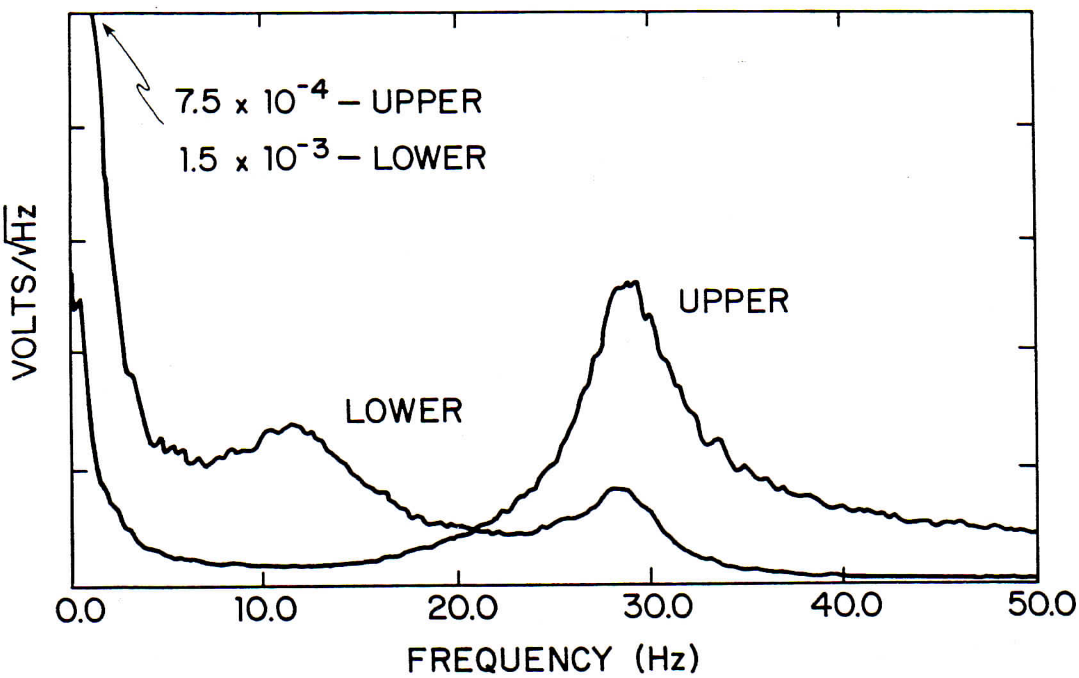

Fig. 4 Measured voltage spectra of the upper and lower position transducers while the rotors are doubly suspended. Note that the scale for the lower suspension is a factor 20 larger than the scale of Fig. 2. The analyzer bandwidth was 300 mHz.

compared to the spectrum of the upper suspension shown in Fig. 1. The amplitude for frequencies less than 8 Hz increased due to the coupling with the lower rotor.

The spectrum of the lower suspension changed considerably. The amplitude of the resonance peak is at least ten times larger than when singly suspended and has shifted down in frequency from 14 Hz to 11 Hz compared with the spectrum of the single lower suspension in Fig. 2. The increase in amplitude is presumed to be caused by the vertical motion of the upper rotor driving the lower rotor. The coupling between the rotors causes the amplitude at low frequencies to be greatly increased. The lower suspension also has a peak near the resonance frequency of the upper suspension. The presence of this peak is predicted by the equations of the coupled harmonic oscillator model for the double suspension. A shift in the resonant frequency of the lower suspension is expected from the well-known phenomenon of "pulling" of a weak oscillator coupled to a stronger one. The negative value of k_2 causes the stronger upper oscillator to push the resonance frequency of the lower one down. However one of the shifts here is probably also caused by the fact that it is difficult to keep the distance between the lower rotor and the upper rotor the same when they are doubly suspended as it is when the lower rotor is singly suspended, with the upper rotor clamped in position to provide the lifting force.

Graphs of $|A_1|$ and $|A_2|$ of eqs. (4) and (5), shown in Fig. 5, show satisfactory agreement with the measured spectra of Fig. 4. The values used for k_1, $k_2 + k_3$, b_1 and b_3 are approximately equal to those measured from the spectra of Figs. 1 and 2. Approximations were used because of the uncertainties in the measured values of these constants and the difficulty of keeping the equilibrium heights the same as they were in the single suspensions. Note that the spring constant determined from the spectrum of the lower suspension along is the sum of k_2 and k_3. The value for k_2 used in the fitting of the equations (-2.5×10^4 dyne/cm) was chosen because it yielded the best agreement between the calculated response curve and the measured curve of the lower rotor with respect to the location and relative size of the two peaks.

The major deficiencies of the calculated curves is at low frequencies where the amplitudes of the measured spectra are much larger. By observing that this low frequency noise exhibits a slope of about -1 when plotted on log-log scales, it can be assumed that it is 1/f noise. In the response curves in Fig. 5 the masses are assumed to be driven by white noise only.

The upper suspension has at least a 2.0 mm range of stable equilibrium position and a temperature sensitivity measured to be less than 20 µm/°C. The lower suspension has a 1.0 mm range of stable equilibrium position and a temperature sensitively of 65 µm/°C. Consequently the double suspension should be able to withstand a thermal variation of > ± 5°C without becoming unstable. Presently, double suspension runs of > 48 hrs. are made without any adjustments in the

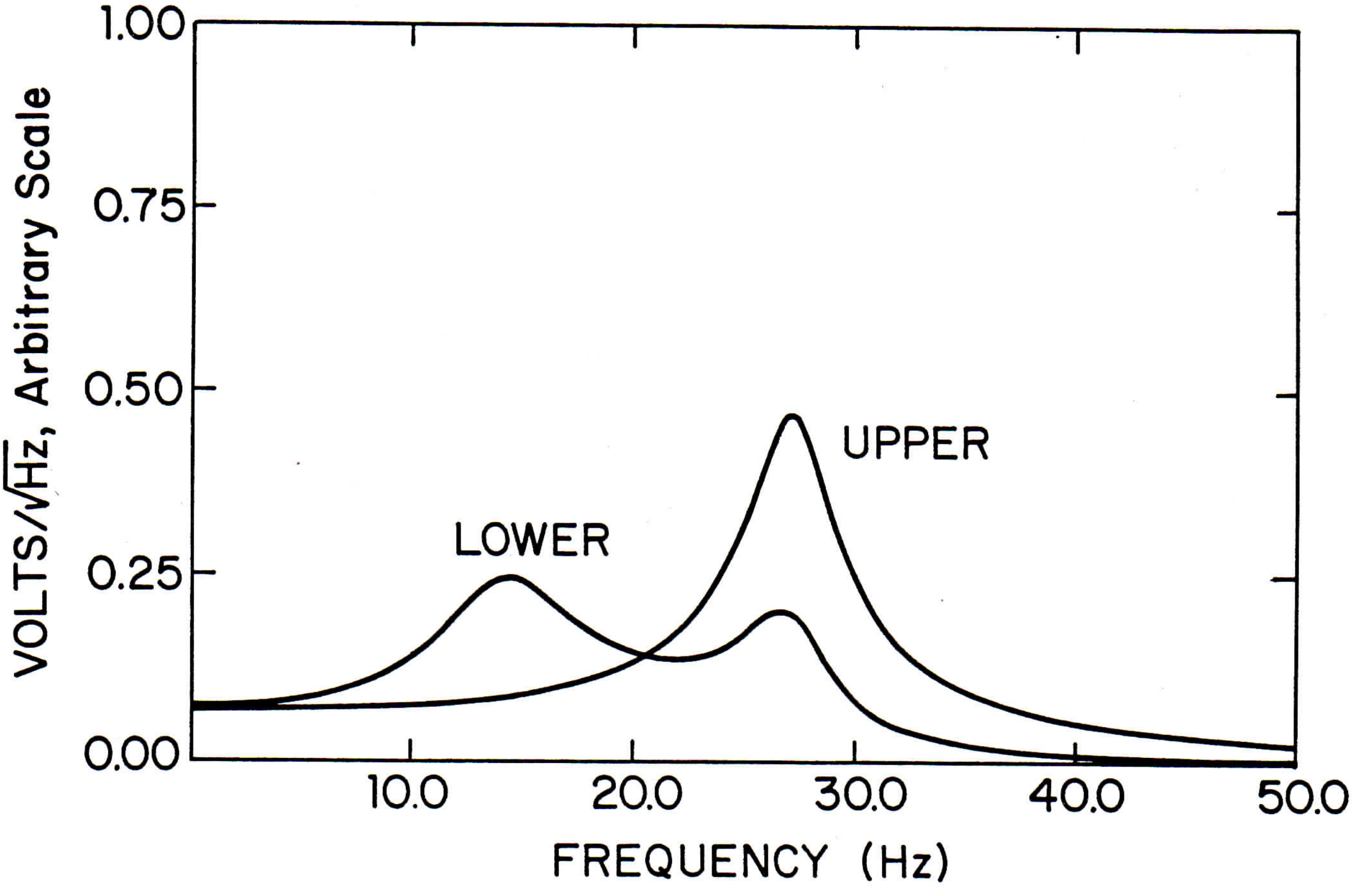

Fig. 5 Response of coupled harmonic oscillators to a white noise driving force as predicted by Eqs. 4 and 5. The amplitudes of the response curves depend on the assumed magnitude of the driving force. The response curves show reasonable agreement with the main features of the spectra of Fig. 4.

servo controls being necessary during the runs. This is much longer than previous limits which were only a few hours.[8] Presumably much longer runs should be possible if the thermal sensitivity of the lower suspension is decreased and the isolation (thermal, vibrational, electrical, etc.) of the system is improved.

V. Conclusion

The double magnetic suspension has been developed and tested as an ultra-stable low-friction double bearing for an inertial clock. This demands the least possible interaction of the lower (inner) rotor with its corotating upper (shroud) rotor. The actual behavior matches reasonably well the predicted mathematic spectral behavior. Temporal and thermal drift have been measured and the complete system stays in suspension without attention for at least several days, in a thermally uncontrolled laboratory.

An improved design of the combined rotor system is being fabricated, with new magnets and more precise machining, as well as many changes in the rotation timing and other features. The new system will be further optimized for stability and reduced inter-rotor interaction.

*Supported in part by NSF Grant PHY80-07948 and NBS Grant G8-9025.

**Present Address: Hanson Laboratories, Stanford University, Palo Alto, CA 94305 (USA)

References

1. Rogers C. Ritter, in Proceedings of the Second Marcel Grossman Meeting Conference on General Relativity, Celebrating the 100th Anniversary of Einstein's Birth, Trieste, Italy, July 1979, ed. R. Ruffini (North Holland, Amsterdam, New York, Oxford, 1982) pp. 1039-1070.

2. Rogers C. Ritter, Journal de Physique, Colloque C-8, supplement au n°12, p. C8-429 to C8-440, (1981).

3. Kurt Lambeck, The Earth's Variable Rotation (Cambridge Univ. Press, Cambridge, 1980).

4. Jiang Zhi, Scienta Sinica, Series B XXV, 326 (1982).

5. J. W. Beams, D. M. Spitzer and J. P. Wade, Rev. Sci. Instrum. 33, 151 (1962).

6. Jesse W. Beams, Sci. Amer. 204, 134 (1961).

7. J. W. Fremery, Phys. Rev. Lett. 30, 753 (1973).

8. J. W. Beams, Rev. Sci. Instrum. 34, 1071 (1963).

9. C. H. Leyh et al, "A Rotational Inertial Clock for Gravitational Redshift Comparisons", in proceedings this symposium.

10. George R. Jones, Rogers C. Ritter and George Thomas Gillies, Metrologia 18, 209 (1982); Rogers C. Ritter and W. Stephen Cheung, "Macroscopic Rotors", proceedings this symposium.

11. George Thomas Gillies, Dissertation, Univ. of Virginia, 1980; George R. Jones, Dissertation, University of Virginia, 1983, University Microfilms, Ann Arbor, Michigan.

12. W. Stephen Cheung et al., Prec. Engrg. 2, 183 (1980).

13. Wah-Kwan Stephen Cheung, Dissertation, Univ. of Virginia, 1982, University Microfilms, Ann Arbor, Mich.

14. Bruce E. Bernard, W. Stephen Cheung and Rogers C. Ritter, Rev. Sci. Instrum. 53, 1743 (1982).

15. Bruce E. Bernard, M. Sc. Thesis, Univ. of Virginia, 1982.

16. J. W. Beams, J. L. Young and J. W. Moore, Jour. Appl. Phys. 17, 886 (1946).

17. W. Stephen Cheung, *et al*., "Analysis of Vertical Magnetic Suspensions," submitted to transactions of IEEE.